Nanoscale Research Letters

NANO EXPRESS Open Access

One-Step In Situ Self-Assembly of Cypress Leaf-Like $Cu(OH)_2$ Nanostructure/Graphene Nanosheets Composite with Excellent Cycling Stability for Supercapacitors

Zhihao Zhai[1], Yuxiu You[1*], Liguo Ma[1], Dongkai Jiang[1], Fanggang Li[1], Hao Yuan[1], Maojun Zheng[1,2*] and Wenzhong Shen[1]

Abstract

Transition metal hydroxides and graphene composite holds great promise to be the next generation of high performance electrode material for energy storage applications. Here we fabricate the cypress leaf-like $Cu(OH)_2$ nanostructure/graphene nanosheets composite through one-step in situ synthesis process, employed as a new type of electrode material for high efficiency electrochemical energy storage in supercapacitors. A solution-based two-electrode system is applied to synthesize $Cu(OH)_2$/graphene hybrid nanostructure, where anodic graphene nanosheets firmly anchor cathodic $Cu(OH)_2$ nanostructure due to the electrostatic interaction. The in situ self-assembly of $Cu(OH)_2$/graphene ensures good structural robustness and the cypress leaf-like $Cu(OH)_2$ nanostructure prompt to form the open and porous morphology. The hybrid structure would facilitate charge transport and effectively mitigate the volume changes during long-term charging/discharging cycles. As a consequence, the $Cu(OH)_2$/graphene composite exhibits the highest capacitance of 317 mF/cm^2 at the current density of 1 mA/cm^2 and superior cyclic stability with no capacitance decay over 20,000 cycles and remarkable rate capability at increased current densities.

Keywords: Cypress leaf-like $Cu(OH)_2$ nanostructure, graphene nanosheets, outstanding cycling performance

Introduction

The ever depletion of fossil fuels and aggravation of environmental pollutions call for urgently exploring sustainable energy sources and developing energy storage technologies to meet application requirements of many electronic devices and hybrid vehicles in our modern society [1, 2]. As a promising energy storage device, supercapacitors (SCs) have attracted much attention in view of their small size, high power density, fast recharge ability, long lifespan and desirable operational safety [3–8] There are two classes of SCs, pseudocapacitors and electrical double layer capacitors (EDLCs), on the basis of energy storage mechanism [9]. Carbon material with many advantages of abundance, non-toxic, large surface area, good conductivity, excellent chemical durability, is a typical electrode material for double-layer capacitors (EDLCs), storing charge in the electric double-layer near electrolyte/electrode surface by electrostatic adsorption [10–16]. However, carbon material generally exhibits a relatively low specific capacitance. By comparison, many inexpensive transition metal hydroxides, such as $Ni(OH)_2$ [17, 18], NiO [19], MnO_2 [20], Co_3O_4 [21] store energy partially relied on fast reversible Faradic redox reactions occurring on the electrode surface, offering much higher pseudo-capacitance [22, 23]. Unfortunately, most of them suffer from the intrinsic poor electric conductivity and undergo huge volume change during electrochemical processes, which results in the poor reversibility and short cycle life [24]. Obviously, to synthesize the high-performance electrode material at a low cost, it is of great significance to combine easily

* Correspondence: youyuxiuphy@163.com; mjzheng@sjtu.edu.cn
[1]Key Laboratory of Artificial Structures and Quantum Control (Ministry of Education), School of Physics and Astronomy, Shanghai Jiao Tong University, Shanghai, China
Full list of author information is available at the end of the article

available transition metal hydroxides with carbon material by a cost-effective and facile fabrication strategy.

Among various transition hydroxides, $Cu(OH)_2$ is one of the most promising electrode material because of its natural abundance, environmentally friendly and fast redox couple [25–27]. Besides the above -mentioned characteristics of most carbon material, graphene has an exceptionally large specific surface area, whose major surfaces are exposed to the electrolyte, exhibiting a high specific capacitance (550 F/g) [28]. To improve the electric conductivity and enhance capacity of electrode, $Cu(OH)_2$ and graphene composite have been designed as electrode, efficiently inhibiting the volume changes of $Cu(OH)_2$ and preventing serious agglomeration and re-stacking of graphene because the typical flexible and robust nature of graphene enable electrode materials to effectively maintain the structural integration [26, 29–31]. Mahanty et al. presented that the reduced graphene oxide/$Cu(OH)_2$ composite, which exhibited a high capacitance of 602 F g^{-1} and good capacitance retention of 88.8% over 5000 cycles. Both specific capacitance and cyclic stability were dramatically enhanced, compared with pristine $Cu(OH)_2$ [26]. Ghasemi et al. prepared Cu_2O-$Cu(OH)_2$-graphene nanocomposite by multiple steps, including electrophoretic deposition and electrodeposition techniques, exhibited specific capacitance of 425 F g^{-1} and maintained about 85% of initial capacitance with a current density of 10 A g^{-1} after 2500 cycles [32]. Although supercapacitive properties have been enhanced in the report, most of these approaches are complicated and expensive. Furthermore, the cycling stability of reported $Cu(OH)_2$/graphene composite for supercapacitance needs to be further improved.

In this work, we report the one-step in situ self-assembly of cypress leaf-like $Cu(OH)_2$ nanostructure/graphene nanosheets composite realizes in a two-electrode system, where graphene nanosheets generate from electrochemical exfoliation of graphite at anode and simultaneously $Cu(OH)_2$ nanostructure forms on Cu foam at cathode. The morphology and structure, together with the interaction between different components of nanocomposite would influence their electrochemical energy storage properties. The transparent few-layer graphene nanosheets firmly anchor on cypress leaf-like $Cu(OH)_2$ surface, forming a porous, open and interconnected structure. This unique hybrid structure is expected to endow this composite fast charge transfer velocity, high electrochemical activity, and excellent stability. As a result, the $Cu(OH)_2$/graphene composite presents excellent electrochemical energy storage performance with high specific capacitance and wonderful cyclic stability over 20,000 cycles, making it an ideal electrode material for high-performance SCs.

Methods Section

Sample Preparation

The copper foam (10 × 15 × 1.6 mm^3, Xiamen Yongchangshuo Electronic Technology Co. Ltd., China) and graphite foil (10 × 15 × 1.0 mm^3, Shanghai Alfa Aesar Chemical Co. Ltd., China) slices were washed in an ultrasonic bath with absolute ethanol and DI water for 15 min respectively [33], afterward the slices were placed in deionized water for later use. As illustrated in Fig. 1, the electrochemical synthesis process was implemented in a two-electrode cell system [9], where graphite foil acts as anode and Cu foam acts as cathode. In order to achieve in situ self-assembly of cypress leaf-like $Cu(OH)_2$ nanostructure/graphene nanosheets composite, the electrolyte is a mixed solution of 0.1 M $(NH_4)_2SO_4$ (100 mL) and $NH_3{\cdot}H_2O$ (3 mL). When the two-electrode cell system was applied to a direct current voltage of 7 V for 1 h, at anode the graphite foil was electrochemically exfoliated and decomposed into a lot of graphene nanosheets and at cathode Cu foam was corroded into cypress leaf-like $Cu(OH)_2$ by $NH_3{\cdot}H_2O$.

$$Cu + 6\,NH_3 + 2\,H_2O \rightarrow \left[Cu(NH_3)_6\right]^{2+} + 2\,OH^- + H_2\uparrow \quad (1)$$

$$Cu^{2+} + 2\,OH^- \rightarrow Cu(OH)_2 \quad (2)$$

Driven by the electric field, the exfoliated graphene nanosheets with residual negative charges at its edge were electrically attracted to the surface of cathodic $Cu(OH)_2$, assembling into this unique porous nanostructure. The resulting cypress leaf-like $Cu(OH)_2$ nanostructure/graphene nanosheets composite was air dried.

Characterizations

The X-ray diffraction (XRD) was carried out on a Rigaku Ultima IV X-ray Diffractometer by Cu Kα radiation with the scan rate of 2°min^{-1} over a 2θ range from 10° to 80°. Raman spectroscopy was acquired on Renishaw in a Via-reflex system, with the excitation source of a laser wavelength (532 nm). We obtain the details of morphology, structure, crystal size, and other parameters by field emission scanning electron microscopy (FESEM, Zeiss Ultra Plus), transmission electron microscope (TEM), and selected-area electron diffraction (SAED) (JEOL JEM-2100F operating at 200 kV). The surface chemical components and valance states of the sample were researched by X-ray photoelectron spectroscopy (XPS).

Electrochemical Measurements

The electrochemical measurements of the $Cu(OH)_2$/graphene composite on Cu foam was implemented in

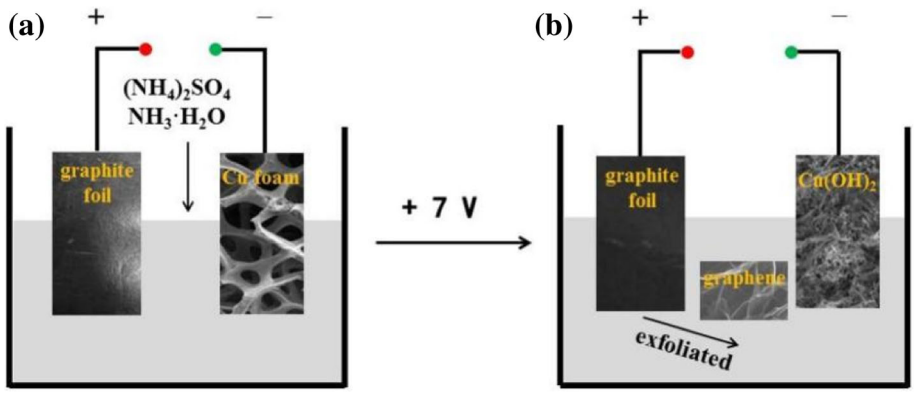

Fig. 1 Schematic diagram of the experimental set-up of one-step in situ self-assembly of $Cu(OH)_2$/graphene composite

a three-electrode configuration with a Ag/AgCl electrode as reference electrode and a Pt plate electrode as counter electrode in 1 M KOH electrolyte. The cyclic voltammetry (CV), and electrochemical impedance spectroscopy (EIS) tests were conducted on PARSTAT 4000. The CV curves and galvanostatic charge-discharge measurements (GCD) were carried out within the potential window from 0 V to 0.6 V, respectively. The GCD and cyclic stability were performed on LAND CT-2001A. The EIS was tested with no bias voltage with the frequency range of 0.01–100 kHz. The area capacitance of the sample was calculated by the following equation:

$$C = \frac{Jt}{\Delta V} \tag{3}$$

, in which C (mF cm^{-2}) represents the area capacitance, J (mA cm^{-2}) is the current density, t (s) is the discharging time, ΔV (V) is the voltage window for cycling tests.

Results and Discussions

The formation and phase purity of $Cu(OH)_2$/graphene composite were studied by X-ray diffraction (Fig. 2a). The peaks marked with an asterisk at 43.4°, 50.6°, and 74.4° are corresponding to the metallic copper (JCPDS 04-0836) of the copper foam. While the diffraction peaks located at 16.7°, 23.9°, 34.2°, 36.0°, 38.3°, 39.9°, 53.5°, 55.3°, 56.5°, and 65.0° are in good agreement with $Cu(OH)_2$ (JCPDS 01-080-0656). The sharp peaks in the diffraction pattern indicate that the synthesis material has good crystallinity and high pure $Cu(OH)_2$ phase. Raman spectroscopy is a significant instrument for characterization of carbon materials. Figure 2b shows the Raman spectrum for the $Cu(OH)_2$/graphene composite. The Raman spectra exhibit three noticeable peaks at 1349 cm^{-1}, 1579 cm^{-1}, and 2715 cm^{-1} corresponding to the D-band, G-band, and 2D-band of graphene, respectively, which confirmed the existence of graphene [9].

Figure 3 displays the morphology and structure of cypress leaf-like $Cu(OH)_2$ nanostructure/graphene nanosheets. As shown in Fig. 3a, a typical FESEM image shows that the $Cu(OH)_2$ nanostructure interweave with

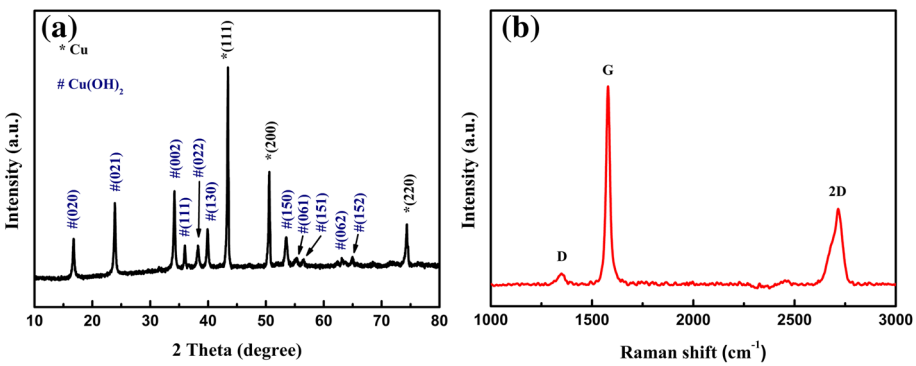

Fig. 2 **a** X-ray diffractogram and **b** Raman spectra of $Cu(OH)_2$/graphene composite

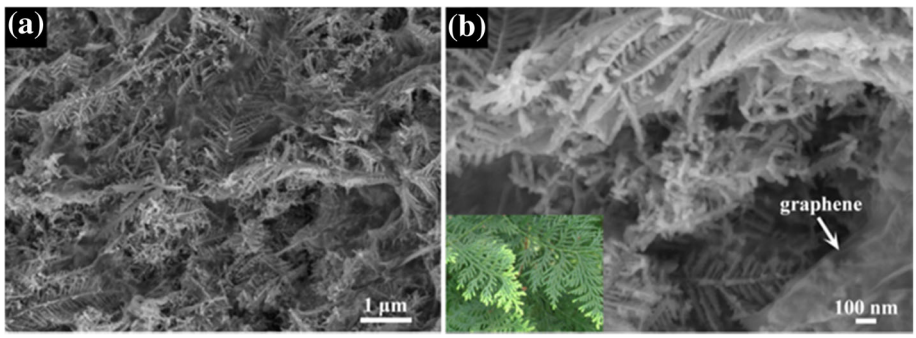

Fig. 3 FESEM images of the $Cu(OH)_2$/graphene composite at **a** low and **b** high magnification

the graphene nanosheets to form a highly open and porous interconnected nanostructure. Figure 3b presents the enlarged FESEM image of some representative $Cu(OH)_2$/graphene composite and indicates that the in situ synthesized $Cu(OH)_2$ composed of short one-dimensional nanorod has a similar morphology of cypress leaf and the graphene nanosheets are ultrathin and transparent. This $Cu(OH)_2$/graphene hybrid nanostructure is expected to have a large surface area, good ion accessibility, and mechanical adhesion.

The detailed nanostructure of the $Cu(OH)_2$/graphene composite is analyzed by TEM. The low magnification TEM image in Fig. 4a shows that the cypress leaf-like $Cu(OH)_2$ nanostructure attached to ultrathin graphene nanosheets, which be consistent with the SEM images. We performed selected area electron diffraction (SAED) of graphene as shown in the inset Fig. 4a. The well-defined diffraction spots and hexagonal diffraction pattern confirm the crystalline structure of the graphene nanosheets obtained via exfoliation from graphene foil. From the high-magnification TEM images (Fig. 4b), we can find the branches of cypress leaf-like $Cu(OH)_2$ nanostructure have an average length of 300 nm and diameter of 15 nm. Moreover, the clearly visible diffraction spots in the SAED pattern (inset of Fig. 4b) reveals that the branch of cypress leaf-like $Cu(OH)_2$ has a good crystallinity. The diffraction spots with a calculated d-spacing of 0.25 nm, 0.22 nm, 0.16 nm, and 0.14 nm can be associated with the (111), (130), (151), and (152) facet of $Cu(OH)_2$. Figure 4c depicts a HRTEM image and the lattice fringe of 0.22 nm is assigned to (130) facet of $Cu(OH)_2$. Observation of clear lattice fringe further confirms the formation of the branches of cypress leaf-like $Cu(OH)_2$ with good crystallinity.

The chemical valence states and element composition are characterized by deconvoluted XPS spectra as presented in Fig. 5. The XPS of Cu 2p is displayed by Fig. 5a. The peak observed at 954.5 eV and 934.6 eV are indexed to Cu $2p_{1/2}$ and Cu $2p_{3/2}$ peaks of Cu^{2+}, respectively, indicating the existence of $Cu(OH)_2$. Due to the Cu foam as substrate, the characteristic peaks at 952.1 eV and 932.3 eV are from Cu $2p_{1/2}$ and Cu $2p_{3/2}$. The C 1s XPS spectrum (Fig. 5b) of $Cu(OH)_2$/graphene is deconvoluted into three peaks: C=O (288.5 eV), C-OH (285.6 eV), and C-C (284.8 eV), respectively. O 1s spectra (Fig. 5c) has two contributions: the two peaks at 531.6

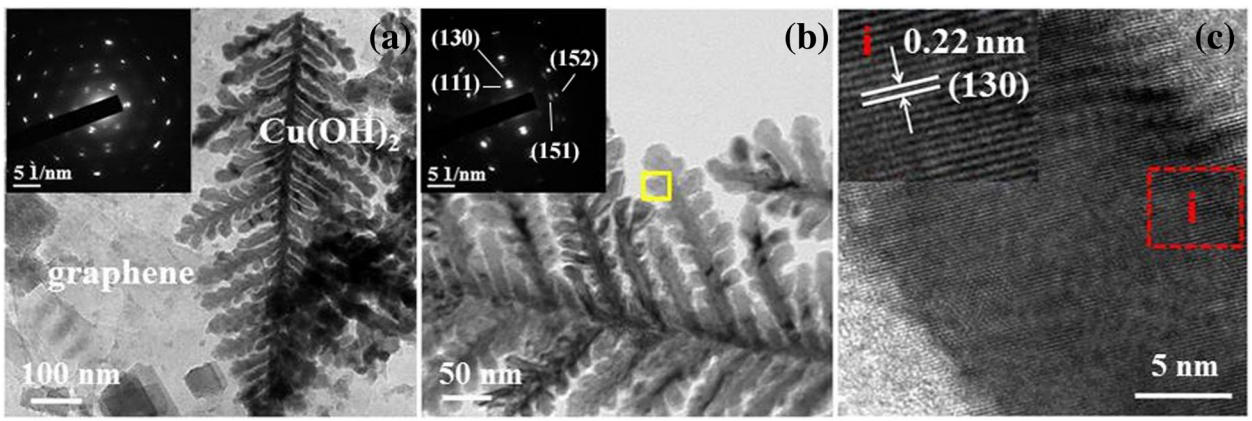

Fig. 4 **a** TEM image of the $Cu(OH)_2$/graphene composite. The inset SAED pattern originates from graphene nanosheets. **b** High-magnification TEM image with the SAED of one branch of cypress leaf-like $Cu(OH)_2$ in the inset. **c** High-resolution TEM image of the marked area in Fig. 4b

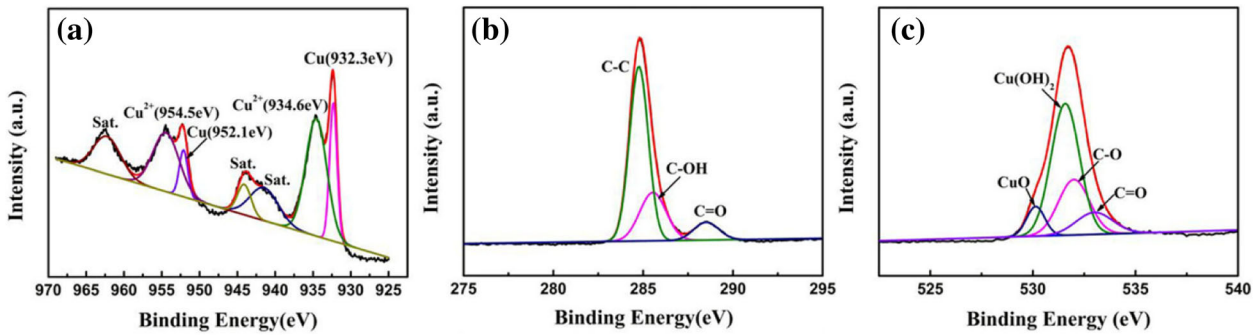

Fig. 5 XPS spectra of **a** Cu 2p, **b** C 1s. and **c** O 1s

eV and 530.1 eV can be assigned to the oxygen species in $Cu(OH)_2$ and CuO, respectively, the other two peaks at 532 eV and 533 eV originates from C-O and C=O, respectively.

The electrochemical charge storage capability of the $Cu(OH)_2$/graphene nanocomposite was investigated by taking them as working electrodes. The cyclic voltammogram (CV) curves of $Cu(OH)_2$/graphene are shown in Fig. 6a, when tested at various scan rates with the range from 5 $mV\,s^{-1}$ to 100 $mV\,s^{-1}$. A pair of well-defined redox peaks is obviously observed in each curve, corresponding to the reversible reaction of $Cu^{2+} \leftrightarrow Cu^{1+}$. The reversible redox reactions can be expressed as [27]

$$2\,Cu(OH)_2 + 2\,e^- \Longleftrightarrow Cu_2O + 2\,OH^- + H_2O \quad (4)$$

With increasing scan rate, CV curves maintain a similar profile and the current response increased, indicating the good rate capability and good reversibility of Faradic reactions [17, 27]. Meanwhile, the oxidation and reduction peak respectively shift to more positive and more negative potentials, due to the limited ion diffusion time or high-electron hopping resistance [34].

Figure 6b displays the area capacitance and galvanostatic charge-discharge curves at different current densities of 1, 2, 4, 8, and 10 $mA\,cm^{-2}$. The galvanostatic

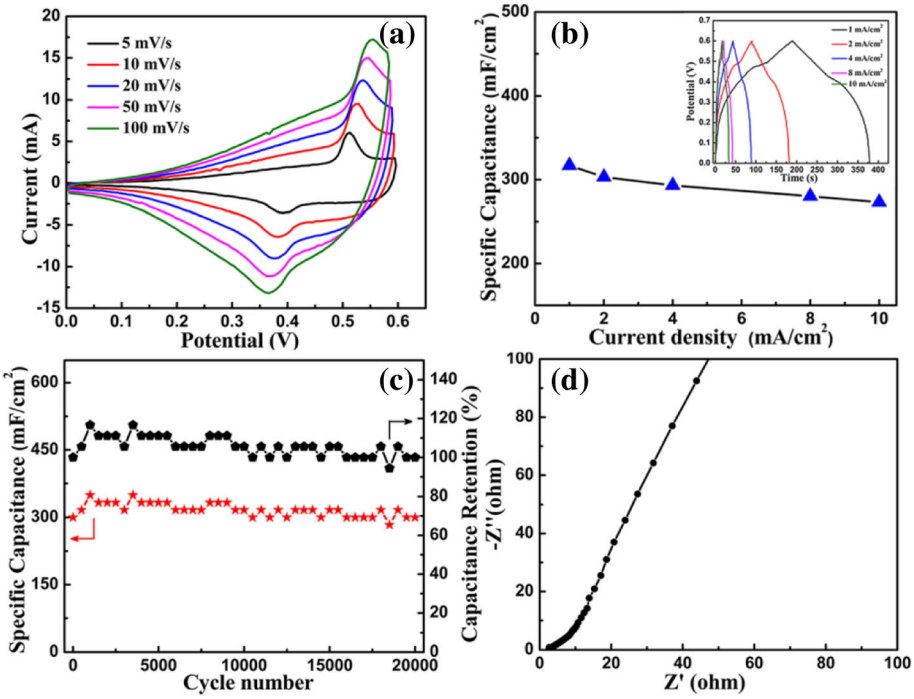

Fig. 6 Electrochemical performance of the $Cu(OH)_2$/graphene composite. **a** CV curves. **b** The specific capacitance and galvanostatic charging/discharging curves. **c** Area capacitance and Coulombic efficiency at a current density of 2 $mA\,cm^{-2}$. **d** Nyquist plot of the $Cu(OH)_2$/graphene

charge-discharge curves of the composite electrode exhibit the typical pseudo-capacitive nature, which finely agrees with its CV curves. The $Cu(OH)_2$/graphene composite achieves the highest area-specific capacitance of 317 mF cm^{-2} at a current density of 1 mA cm^{-2}. The specific capacitance can maintain 303, 293, 280, 273 mF cm^{-2} at different current densities. The $Cu(OH)_2$/graphene nanocomposite electrode shows a good rate capability with only 14% capacitance loss at a high current density of 10 mA cm^{-2}, which can be ascribed to the unique nanostructure in favor of fast and efficient electrolyte ion diffusion and charge transfer [17].

The cycling stability of the $Cu(OH)_2$/graphene nanocomposite electrode was studied by charging-discharging cycling measurements at the constant current density of 2 mA cm^{-2} (Fig. 6c). The specific capacitance till 20,000 cycles keep the initial value of 303 mF cm^{-2} with 100% retention, exhibiting the outstanding cycling performance. Moreover, the Coulombic efficiency can maintain 100% which further demonstrates that the electrode possesses good electrochemical stability. Form Fig. 6d, the intercept value about 2.35 on real axis represents the internal resistance (R_S) in high-frequency area. The slightly high internal resistance is mainly attributed to the inherent resistance of active material, due to the natural defect in electric conductivity of $Cu(OH)_2$. The slope of the Nyquist plot reflects the Warburg impedance, which demonstrates a low electrolyte diffusion resistance. The open porous $Cu(OH)_2$/graphene nanocomposite nanostructure with large surface area endows the electrode with abundant reactive sites and shorten ion diffusion path.

The excellent electrochemical energy storage properties of the $Cu(OH)_2$/graphene nanocomposite are ascribed to the following reasons: (i) the 3D Cu foam substrate analogous to the reported Ni foam also has many advantages of high-electric conductivity, large surface area, microscale pores and many flow channels, providing the active material with high mass loading, and large effective surface area [35, 36]; (ii) due to the cypress leaf-like $Cu(OH)_2$ synthesized by in situ oxidation of Cu foam, this binder-free electrode not only reduce the dead volume effect and the internal resistance but also prompt the effective charge transfer and fast redox reactions [37, 38]; (iii) the electric conductivity of the $Cu(OH)_2$ can be improved by assembling with graphene, facilitating the electrolyte ions diffusion and electron transport [39]; (iv) to some extent, the volume changes of $Cu(OH)_2$ and especially the agglomeration of graphene all can be alleviated, increasing the stability of both nanostructure and electrochemical performance during continuous charge-discharge processes [29]; (v) the unique open, porous, and interconnected nanostructure can reserve electrolyte ions to ensure the sufficient redox reactions particularly at high current densities [40].

Conclusions

We have adopted a simple electrochemical method based on solution to in situ synthesize cypress leaf-like $Cu(OH)_2$ nanostructure/graphene nanosheets on Cu foam serving as a promising electrode for supercapacitors. This novel hybrid nanostructure endows the $Cu(OH)_2$/graphene nanocomposite with abundant redox reactions, good charge transfer, and short electrolyte ion diffusion pathway. When evaluated as the electrode material for supercapacitors, the $Cu(OH)_2$/graphene nanocomposite demonstrates high reversible capacitance of 317 mF cm^{-2} and excellent stability with 100 % retention over 20,000 cycles at current densities of 2 mA cm^{-2} and remarkable rate capability at increased current densities. This synthesis method will open a new door for the facile fabrication of other hydroxides and provides an effective strategy for remarkable electrochemical energy storage devices.

Abbreviations

CV: Cyclic voltammetry; EDLCs: Electrical double layer capacitors; EIS: Electrochemical impedance spectroscopy; FESEM: Field emission scanning electron microscopy; GCD: Galvanostatic charge-discharge measurements; HRTEM: High- resolution transmission electron microscopy; SAED: Selected-area electron diffraction; SCs: Supercapacitors; SEM: Scanning electron microscopy; TEM: Transmission electron microscopy; XPS: X-ray photoelectron spectroscopy; XRD: X-ray diffraction

Acknowledgements

We gratefully acknowledge the support of this work by the National Natural Science Foundation of China (grant nos. 11174197 and 11574203).

Availability of Data and Materials

The datasets used during the current study are available from the corresponding author on reasonable request.

Authors' Contributions

ZZH performed the experiments. ZZH, YYX, and MLG designed the experiment. ZZH, YYX, JDK, LFG, and YH analyzed the data. ZZH wrote the paper. ZMJ, SWZ checked the paper. All authors read and approved the final manuscript.

Competing Interests

The authors declare that they have no competing interests.

Publisher's Note

Author details

[1]Key Laboratory of Artificial Structures and Quantum Control (Ministry of Education), School of Physics and Astronomy, Shanghai Jiao Tong University, Shanghai, China. [2]Collaborative Innovation Center of Advanced Microstructures, Nanjing University, Nanjing, China.

Received: 11 March 2019 Accepted: 6 May 2019
Published online: 17 May 2019

References

1. Cao XY, Cui L, Liu BP, Liu Y, Jia DD, Yang WR, Razal JM, Liu JQ (2019) Reverse synthesis of star anise-like cobalt doped Cu-MOF/$Cu_{2+1}O$ hybrid materials based on $Cu(OH)_2$ precursor for high performance supercapacitors. J Mater Chem A 7:3815–3827

2. He D, Wang GD, Liu GL, Bai JH, Suo H, Zhao C (2017) Facile route to achieve mesoporous $Cu(OH)_2$ nanorods on copper foam for high-performance supercapacitor electrode. J Alloys Comp 699:706–712
3. Xiao X, Song HB, Lin SZ, Zhou Y, Zhan XJ, Hu ZM, Zhang Q, Sun JY, Yang B, Li TQ, Jiao LY, Zhou J, Tang J, Gogotsi Y (2016) Scalable salt-templated synthesis of two-dimensional transition metal oxides. Nat Comm 7:11296
4. Xie JQ, Ji YQ, Kang JH, Sheng JL, Mao DS, Fu XZ, Sun R, Wong CP (2019) In situ growth of $Cu(OH)_2$@FeOOH nanotube arrays on catalytically deposited Cu current collector patterns for high-performance flexible in-plane micro-sized energy storage devices. Energy Environ Sci 12:194
5. Wei JS, Ding H, Zhang P, Song YF, Chen J, Wang YG, Xiong HM (2016) Carbon Dots/$NiCo_2O_4$ Nanocomposite with Various Morphologies for High Performance Supercapacitors. Small 12:5927–5934
6. Choi KH, Ahn DB, Lee SY (2018) Current status and challenges in printed batteries: Toward form factor-free, monolithic integrated power sources. ACS Energy Lett 3:220–236
7. Li L, Fu CW, Lou Z, Chen S, Han W, Jiang K, Chen D, Shen GZ (2017) Flexible planar concentric circular micro-supercapacitor arrays for wearable gas sensing application. Nano Energy 41:261–268
8. Yu PP, Zhang ZM, Zheng LX, Teng F, Hu LF, Fang XS (2016) A Novel Sustainable Flour Derived Hierarchical Nitrogen-Doped Porous Carbon/Polyaniline Electrode for Advanced Asymmetric Supercapacitors. Adv Energy Mat 6:1601111
9. Ma LG, Zheng MJ, Liu SH, Li Q, You YX, Wang FZ, Ma L, Shen WZ (2016) Synchronous exfoliation and assembly of graphene on 3D $Ni(OH)_2$ for supercapacitors. Chem Commun 52:13373–13376
10. Huang L, Chen D, Ding Y, Feng S, Wang ZL, Liu M (2013) Nickel-cobalt hydroxide nanosheets coated on $NiCo_2O_4$ nanowires grown on carbon fiber paper for high-performance pseudocapacitors. Nano Lett 13:3135–3139
11. Wang YG, Song YF, Xia YY (2016) Electrochemical capacitors: mechanism, materials, systems, characterization and applications. Chem Soc Rev 45:5925–5950
12. Simon P, Gogotsi Y, Dunn B (2014) Where do batteries end and supercapacitors begin? Science 343:1210–1211
13. Salanne M, Rotenberg B, Naoi K, Kaneko K, Taberna PL, Grey PC, Dunn B, Simon P (2016) Efficient storage mechanisms for building better supercapacitors. Nat Energy 1:16070
14. Gao N, Fang XS (2015) Synthesis and development of graphene–inorganic semiconductor nanocomposites. Chem Rev 115(16):8294–8343
15. Xie KJ, Zhang MM, Yang Y, Zhao L, Qi W (2018) Synthesis and supercapacitor performance of polyaniline/nitrogen-doped ordered mesoporous carbon composites. Nanoscale Res Lett 13:163
16. Ouyang WX, Teng F, He JH, Fang XS (2019) Enhancing the photoelectric performance of photodetectors based on metal oxide semiconductors by charge-carrier engineering. Adv Func Mat 29:1807672
17. Xiong XH, Ding D, Chen DC, Waller G, Bu YF, Wang ZX, Liu ML (2015) Three-dimensional ultrathin $Ni(OH)_2$ nanosheets grown on nickel foam for high-performance supercapacitors. Nano Energy 11:154–161
18. Tang Z, Tang CH, Gong H (2012) A high energy density asymmetric supercapacitor from nano-architectured $Ni(OH)_2$/carbon nanotube electrodes. Adv Funct Mat 22:1272–1278
19. He D, Liu G, Pang A, Jiang Y, Suo H, Zhao C (2017) A high-performance supercapacitor electrode based on tremella-like NiC_2O_4@NiO core/shell hierarchical nanostructures on nickel foam. Dalton Transac 46(6):1857–1863
20. Zhang GD, Liu XC, Wang YH, Liu CZ, Xing SX (2017) Achieving MnO_2 nanosheets through surface redox reaction on nickel nanochains for catalysis and energy storage. Chemistry A Eur J 23:5557–5564
21. Qorbani M, Naseri N, Moshfegh AZ (2015) Hierarchical Co_3O_4/$Co(OH)_2$ nanoflakes as a supercapacitor electrode: experimental and semi-empirical model. ACS Appl Mat Inter 7:11172–11179
22. Jiang WC, Yu DS, Zhang Q, Goh K, Wei L, Yong YL, Jiang RR, Wei J, Chen Y (2015) Ternary hybrids of amorphous nickel hydroxide-carbon nanotube-conducting polymer for supercapacitors with high energy density, excellent rate capability, and long cycle life. Adv Funct Mat 25:1063–1073
23. Chai Z, Jiang CH (2019) Electrochemical/chemical growth of porous $(Ni,Co,Cu)(OH)_2$ as an electrode material: Ternary Ni-Co-Cu nanocrystalline films corroded in neutral salt spray. Electrochimica Acta 294:11–21
24. Gao S, Sun Y, Lei F, Liang L, Liu J, Bi W, Pan B, Xie Y (2014) Ultrahigh energy density realized by a single-layer beta-$Co(OH)_2$ all-solid-state asymmetric supercapacitor. Angew Chem Int Ed 53:12789–12793
25. Chen JZ, Xu JL, Zhou S, Zhao N, Wong CP (2015) Facile and scalable fabrication of three-dimensional $Cu(OH)_2$ nanoporous nanorods for solid-state supercapacitors. J Mat Chem A 3:17385–17391
26. Pramanik A, Maiti S, Mahanty S (2015) Reduced graphene oxide anchored $Cu(OH)_2$ as a high performance electrochemical supercapacitor. Dalton Transac 44:14604–14612
27. Lei SJ, Liu Y, Fei LF, Song RB, Lu W, Shu LL, Mak CL, Wang Y, Huang HT (2016) Commercial Dacron cloth supported $Cu(OH)_2$ nanobelt arrays for wearable supercapacitors. J Mat Chem A 4:14781–14788
28. Liu C, Yu Z, Neff D, Zhamu A, Jang BZ (2010) Graphene-based supercapacitor with an ultrahigh energy density. Nano Lett 10:4863–4868
29. Kim MS, Lim E, Kim S, Jo C, Chun J, Lee J (2017) General synthesis of N-doped macroporous graphene-encapsulated mesoporous metal oxides and their application as new anode materials for sodium-ion hybrid supercapacitors. Adv Func Mat 27:1603921
30. Zhou GM, Wang DW, Li F, Zhang LL, Li N, Wu ZS, Wen L, Lu GQ, Cheng HM (2010) Graphene-wrapped Fe_3O_4 anode material with improved reversible capacity and cyclic stability for lithium ion batteries. Chem Mat 22:5306–5313
31. Gao GX, Wu HB, Lou XW (2014) Citrate-assisted growth of $NiCo_2O_4$ nanosheets on reduced graphene oxide for highly reversible lithium storage. Adv Energy Mat 4:1400422
32. Ghasemi S, Jafari M, Ahmadi F (2016) Cu_2O-$Cu(OH)_2$-graphene nanohybrid as new capacitive material for high performance supercapacitor. Electrochimica Acta 210:225–235
33. He D, Wan J, Suo H, Zhao C (2016) In situ facile surface oxidation method prepared ball of yarn-like copper oxide hierarchical microstructures on copper foam for high performance supercapacitor. Mat Lett 185:165–168
34. You YX, Zheng MJ, Ma LG, Yuan XL, Zhang B, Li Q, Wang FZ, Song JN, Jiang DK, Liu PJ, Ma L, Shen WZ (2017) Galvanic displacement assembly of ultrathin Co_3O_4 nanosheet arrays on nickel foam for a high-performance supercapacitor. Nanotechnology 28:105604
35. Yuan CZ, Yang L, Hou LR, Shen LF, Zhang XG, Lou XW (2012) Growth of ultrathin mesoporous Co_3O_4 nanosheet arrays on Ni foam for high-performance electrochemical capacitors. Energy Environ Sci 5:7883–7887
36. Zhang X, Zhao Y, Xu C (2014) Surfactant dependent self-organization of Co_3O_4 nanowires on Ni foam for high performance supercapacitors: from nanowire microspheres to nanowire paddy fields. Nanoscale 6:3638–3646
37. Wu SX, Hui KS, Hui KN, Kim KH (2016) Ultrathin porous NiO nanoflake arrays on nickel foam as an advanced electrode for high performance asymmetric supercapacitors. J Mat Chem A 4:9113–9123
38. Xu PP, Ye K, Du MM, Liu JJ, Cheng K, Yin JL, Wang GL, Cao DX (2015) One-step synthesis of copper compounds on copper foil and their supercapacitive performance. RSC Adv 5:36656–36664
39. Zhao B, Liu P, Zhuang H, Jiao Z, Fang T, Xu WW, Lu B, Jiang Y (2013) Hierarchical self-assembly of microscale leaf-like CuO on graphene sheets for high-performance electrochemical capacitors. J Mat Chem A 1:367–373
40. Zhang YQ, Li L, Shi SJ, Xiong QQ, Zhao XY, Wang XL, Gu CD, Tu JP (2014) Synthesis of porous Co_3O_4 nanoflake array and its temperature behavior as pseudo-capacitor electrode. J Power Sour 256:200–205